Heterometallic Molecular Squares and Polymers Based On Self-Assembly Reactions of Multiply Bonded Dirhenium Complexes

Jitendra K. Bera,[a] John Bacsa,[a] Bradley W. Smucker,[a] and Kim R. Dunbar*[a]

Keywords: Self-assembly / Polymers / Supramolecular chemistry / Rhenium / Multiple bonds

Self-assembly reactions of the triply-bonded dirhenium complex *cis*-$[Re_2Cl_2(dppm)_2(O_2CC_5H_4N\text{-}4)_2]$ with *cis*-protected Pt^{II} and Zn^{II} precursors have produced heterometallic squares. Analogous reactions with $Ag(O_3SCF_3)$, *cis*-$[Re_2Cl_4(O_2CCH_3)_2(H_2O)_2]$ and $[Rh_2(O_2CCH_3)_4]$ have yielded mixed-metal polymeric structures. These results demonstrate that the isonicotinate ligand is useful for accessing heterometallic structures involving metal–metal bonded complexes.

Introduction

The assembly of metal-based units into supramolecular structures may furnish interesting conducting,[1] magnetic,[2] optical,[3] or catalytic properties.[4] Among the complexes that have been synthesized in this vein are dimetal (M_2) "lantern" complexes as building blocks for homometallic supramolecular assemblies, efforts that have largely focused on the use of dicarboxylic acids.[5] In addition, edge-sharing bi-octahedral dirhenium units can be linked by cyanide and thiocyanate to yield mixed metal Re_4Pd_2, Re_2Ag, Re_2W, Re_2Pt, and Re_2Rh complexes.[6] Recently, we reported a new type of self-assembly reaction that affords molecules with both M_2 and M′ units. The isonicotinate ligand was used as it binds to three metals (Scheme 1). Specifically, the precursor molecule *cis*-$[Re_2Cl_2(dppm)_2(O_2CC_5H_4N\text{-}4)_2]$ (**1**) was synthesized and treated with *cis*-$[Pt(dbbpy)(Otf)_2]$ (dbbpy = 4,4′-di-*tert*-butyl-2,2′-bipyridine; Otf = O_3SCF_3) to yield a molecular square composed of alternating dirhenium and platinum corners.[7] Herein we report further reactions of **1** with various metal complexes to yield a new heterometallic molecular square with alternating Re_2 and Zn corners and three open-chain polymers consisting of 1:1 Re_2/Ag, Re_2/Re_2, and Re_2/Rh_2 units.

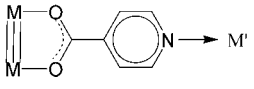

Scheme 1

[a] Department of Chemistry, Texas A&M University, College Station, Texas 77842-3012 (USA)
Fax: (internat.) + 1-979-845-7177
E-mail: dunbar@mail.chem.tamu.edu

Results and Discussion

The molecular structure of complex **1** involves orthogonally disposed isonicotinate groups with two dangling nitrogen donors available for further coordination. Reactions of **1** with *cis* and *trans* accessible transition metal precursors can, in principle, generate various cyclic and open-frame oligomers as well as polymers (Scheme 2). Self-assembly reactions typically yield one major product in a high yield as dictated by a combination of enthalpic and entropic contributions. Here, various building blocks have been employed in reactions of **1**, including $[Pt(dbbpy)(O_3SCF_3)_2]$, $ZnCl_2$, $Ag(O_3SCF_3)$, *cis*-$[Re_2Cl_4(O_2CCH_3)_2(H_2O)_2]$, and $[Rh_2(O_2CCH_3)_4]$, all of which have at least two positions available for facile substitution, but differ in the geometry and disposition of the available metal binding sites. *Hybrid* molecular squares $[\{cis\text{-}Re_2(O_3SCF_3)_2(dppm)_2(O_2CC_5H_4N\text{-}4)_2\}\{Pt(dbbpy)\}]_2(O_3SCF_3)_4$ (**2**) and $[\{cis\text{-}Re_2Cl_2(dppm)_2(O_2CC_5H_4N\text{-}4)_2\}\{ZnCl_2\}]_2$ (**3**), composed of alternating $Re_2^{II,II}$ and M^{II} (M = Pt and Zn) corners, have been isolated from the reactions of **1** with $[Pt(dbbpy)(O_3SCF_3)_2]$[7] and $ZnCl_2$, respectively. In contrast, the reactions of **1** with $Ag(O_3SCF_3)$, *cis*-$[Re_2Cl_4(O_2CCH_3)_2(H_2O)_2]$ and $[Rh_2(O_2CCH_3)_4]$ yield open-chain polymeric structures $[\{cis\text{-}Re_2(OReO_3)_2(dppm)_2(O_2CC_5H_4N\text{-}4)_2\}\{Ag{\cdot}ReO_4\}]_\infty$ (**4**), $[\{cis\text{-}Re_2Cl_2(dppm)_2(O_2CC_5H_4N\text{-}4)_2\}\{cis\text{-}Re_2Cl_4(O_2CCH_3)_2\}]_\infty$ (**5**), and $[\{cis\text{-}Re_2Cl_2(dppm)_2(O_2CC_5H_4N\text{-}4)_2\}\{Rh_2(O_2CCH_3)_4\}]_\infty$ (**6**), respectively. These reactions are essentially instantaneous as judged by the rapid formation of insoluble solids. Crystals of complexes **3**–**6** were obtained by slow diffusion. Regardless of the ratio of complex **1** and the metal precursors, the isolated products are essentially the same. The new compounds **3**–**6** are insoluble in common organic solvents, which prevents measurements of their physical properties in solution.

  DOI: 10.1002/ejic.200300268

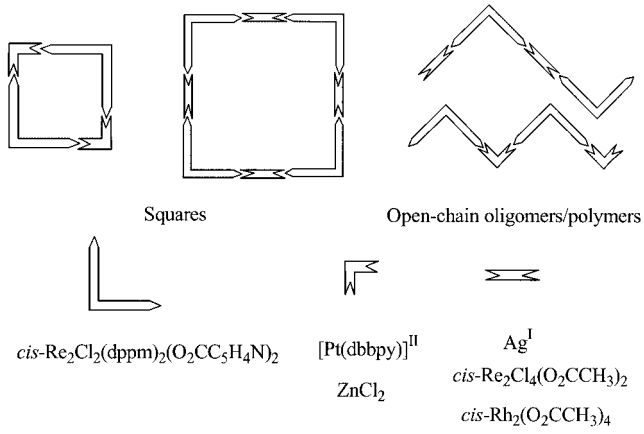

Scheme 2

Complex **3**·10($C_2H_4Cl_2$)·11(CH_3OH)·(H_2O) is a molecular square consisting of alternating $(dppm)_2Re_2^{II}$ and $Zn^{II}Cl_2$ units at the vertices and isonicotinate ligands along the edges (Figure 1). Selected bond lengths and angles are provided in Table 1. The square is considerably distorted, as evidenced by the Zn···Zn diagonal distance of 11.881(5) Å whereas the diagonal defined by the midpoints of the two Re_2 units is 13.608(3) Å. These distances are strikingly similar to the corresponding values in complex **2** (11.971(3) and 13.263(3) Å], the structure of which is identical to complex **3** except that the $ZnCl_2$ corners are replaced by Pt(dbbpy) units (Figure 2). The Re−Re [2.318(1) Å] and the Re−P [2.387(4)−2.412(3) Å], Re−O [2.133(8)−2.160(9) Å], and Re−Cl distances [2.513(3) and 2.523(3) Å] are similar to the corresponding distances in the precursor complex **1**. The vertex angle subtended by the Re_2 units is less than the ideal 90° [O1−Re2−O3 80.6(3)° and O2−Re1−O4 80.0(3)°]. The coordination environment around Zn is best described as distorted tetrahedral. The N1−Zn1−N2 vertex angle is 101.0(5)° while Cl3−Zn1−Cl4 is significantly larger [122.8(2)°], presumably due to non-bonded repulsions between the adjacent chlorine atoms.

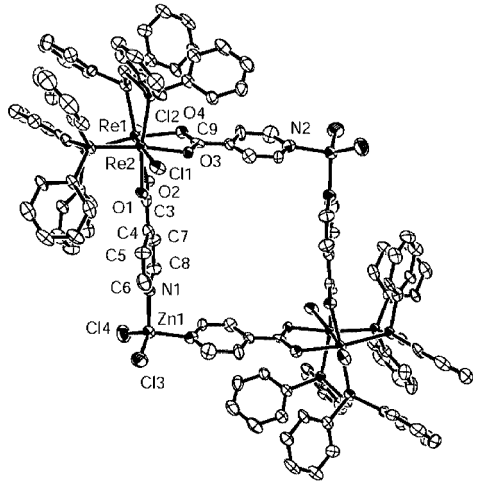

Figure 1. ORTEP representation of the neutral molecular square [{*cis*-$Re_2Cl_2(dppm)_2(O_2CC_5H_4N\text{-}4)_2$}{$ZnCl_2$}]$_2$ in **3**·10($C_2H_4Cl_2$)·11(CH_3OH)·(H_2O) with important atoms labeled. Thermal ellipsoids are at the 50% probability level; hydrogen atoms have been omitted for clarity

Table 1. Selected bond lengths [Å] and angles [deg] for **3**

Bond lengths			
Re1−Re2	2.3175(10)	Re2−O1	2.133(8)
Re1−P2	2.402(3)	Re2−P1	2.394(4)
Re1−P4	2.387(4)	Re2−P3	2.412(3)
Re1−O2	2.160(9)	Zn1−N1	2.041(12)
Re1−O4	2.149(9)	Zn1−N2	2.052(13)
Re1−Cl2	2.513(3)	Zn1−Cl3	2.232(5)
Re2−Cl1	2.523(3)	Zn1−Cl4	2.202(5)
Bond angles			
O4−Re1−O2	80.0(3)	N1−Zn1−N2	101.0(5)
O4−Re1−P4	95.3(3)	N1−Zn1−Cl4	107.8(4)
Re2−Re1−P4	98.71(8)	N2−Zn1−Cl4	110.2(4)
O2−Re1−P2	89.8(3)	N1−Zn1−Cl3	106.1(4)
Re2−Re1−P2	96.06(8)	N2−Zn1−Cl3	106.8(4)
P4−Re1−P2	94.12(12)	Cl4−Zn1−Cl3	122.8(2)

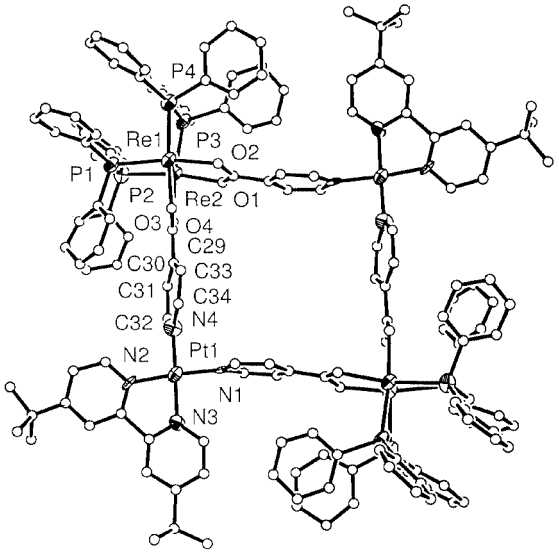

Figure 2. ORTEP representation of the molecular square [*cis*-$Re_2(dppm)_2(O_2CC_5H_4N\text{-}4)_2Pt(dbbpy)]_2$ with important atoms labeled. Thermal ellipsoids are at the 50% level except for the carbon and oxygen atoms which are represented as circles of arbitrary radius. Note that the C, O, F, and S atoms of the triflate anions are axially coordinated, and the hydrogen atoms are removed for clarity

A cyclic voltammetric study of **2** in a 0.1 M nBu_4NPF_6/CH_2Cl_2 solution reveals weak electronic coupling between the dirhenium units through the Pt centers ($\Delta E_{1/2}$ = 130 mV; K_c = 158). The extent of coupling is similar to that estimated for complexes in which dirhenium units are connected by terephthalate ligands.[5]

In complex **4**, the structure of which has been confirmed by X-ray diffraction, the axial chloride ligands have, surprisingly, been replaced by $[ReO_4]^-$ ions. Moreover, it does not contain an outer-sphere triflate anion, rather a second $[ReO_4]^-$ unit is located in the interstices. The $[ReO_4]^-$ anion is a result of oxidative decomposition of **1**, which also explains the relatively low yield of complex **4**. The intense IR

resonances seen between 890 and 950 cm^{-1} indicate ν(Re−O) stretches.

The cationic $[\{cis\text{-}Re_2(OReO_3)_2(dppm)_2(O_2CC_5H_4N\text{-}4)_2\}\{Ag\}]^+$ repeat unit in the crystal structure of **4**·1.5($C_2H_4Cl_2$)·2(CH_3OH) (Figure 3) and selected distances and angles (Table 2) are given here. Each of the $\{Re_2(OReO_3)_2(dppm)_2(O_2CC_5H_4N\text{-}4)_2\}$ units is connected by Ag^I ions.[8] The *anti* orientation of one set of the isonicotinate ligands in adjacent dirhenium units results in a zig-zag pattern for the polymeric structure (see Figure 4, a). The axial positions of the Re_2 unit in complex **4** are occupied by the $[ReO_4]^-$ anion (instead of the original Cl^- ion in **1**) which leads to a slightly shorter Re−Re distance [2.2850(13) Å] as compared to **1** [2.3271(4) Å]. All metrical parameters involving the dirhenium units are typical of other dirhenium−diphosphane complexes.[9] The two-coordinate Ag^I ion is in a nearly linear geometry (N6−Ag1−N18 172.3(8)°] with Ag1−N6 and Ag1−N18 distances of 2.130(18) and 2.128(18) Å, respectively.

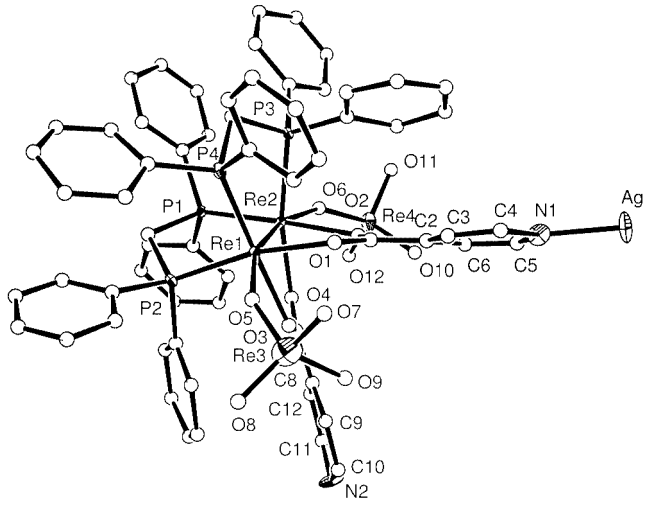

Figure 3. ORTEP representation of the repetitive cationic fragment $[\{cis\text{-}Re_2(OReO_3)_2(dppm)_2(O_2CC_5H_4N\text{-}4)_2\}\{Ag\}]^+$ in **4**·1.5($C_2H_4Cl_2$)·2(CH_3OH) with important atoms labeled. Thermal ellipsoids are at the 40% level except for the carbon and oxygen atoms which are represented as circles of arbitrary radius. Hydrogen atoms have been omitted for clarity

As the complexes *cis*-$[Re_2Cl_4(O_2CCH_3)_2(H_2O)_2]$[10] and $[Rh_2(O_2CCH_3)_4]$[11] engage in axial interactions, they were used here as linkers for complex **1**. Although structurally similar, the difference in the lengths of the quadruple bond in the dirhenium complex [2.224(5) Å] and the single bond in the dirhodium compound [2.403(2) Å] allowed us to vary the linker length. The axial water ligands in *cis*-$[Re_2Cl_4(O_2CCH_3)_2(H_2O)_2]$ are readily replaced by the nitrogen atoms of the isonicotinate ligands in complex **1**. Each of the $\{cis\text{-}Re_2Cl_2(dppm)_2(O_2CC_5H_4N\text{-}4)_2\}$ moieties is coordinated to two different $\{cis\text{-}Re_2Cl_4(O_2CCH_3)_2\}$ units. The isonicotinate ligands of neighboring $\{cis\text{-}Re_2Cl_2(dppm)_2(O_2CC_5H_4N\text{-}4)_2\}$ units are *anti*, leading to a zig-zag chain structure with alternating triply bonded $Re_2^{II,II}$ and quadruply bonded $Re_2^{III,III}$ units (Figure 4, b). A portion of the polymer, namely the $[\{cis\text{-}Re_2Cl_2(dppm)_2(O_2CC_5H_4N\text{-}4)_2\}\{cis\text{-}Re_2Cl_4(O_2CCH_3)_2\}]$ unit, is depicted in Figure 5. Selected bond lengths and angles are provided in Table 3. The Re−Re of 2.3143(9) Å, Re−P [2.371(4)−2.410(4) Å], Re−Cl [2.530(4), and 2.538(4) Å] are all typical of triply bonded dirhenium complexes with similar ligands.

Table 2. Selected bond lengths [Å] and angles [deg] for **4**

Bond lengths			
Re2−Re1	2.2850(13)	Re1−O3	2.133(14)
Ag1−N6	2.13(2)	Re1−O5	2.22(2)
Ag1−N18	2.128(18)	Re2−P1	2.401(5)
Re2−O2	2.120(13)	Re2−P3	2.419(5)
Re2−O4	2.147(13)	Re1−P2	2.405(6)
Re2−O9	2.230(14)	Re1−P4	2.408(6)
Re1−O1	2.133(13)		
Bond angles			
N6−Ag1−N18	172.3(8)	O1−Re1−O3	79.4(5)
O2−Re2−O4	79.4(5)	O1−Re1−O5	78.4(6)
O2−Re2−O9	80.9(5)	O3−Re1−O5	77.9(6)
O4−Re2−O9	80.2(5)	O1−Re1−P2	168.9(4)
O2−Re2−P1	169.5(4)	O3−Re1−P2	90.1(4)
O4−Re2−P1	94.1(4)	O5−Re1−P2	96.0(5)
O9−Re2−P1	90.0(4)	O1−Re1−P4	95.6(4)
O2−Re2−P3	89.9(4)	O3−Re1−P4	171.2(4)
O4−Re2−P3	168.7(4)	O5−Re1−P4	94.0(5)
O9−Re2−P3	94.4(4)	P2−Re1−P4	94.4(2)
P1−Re2−P3	95.83(18)		

The Re(1)−Re(2) [2.244(1) Å] in the $\{Re_2Cl_4(O_2CCH_3)_2\}$ unit is characteristic of a Re−Re quadruple bond, and is slightly longer than the Re−Re bond [2.224(5) Å] in *cis*-$[Re_2(O_2CCH_3)_2Cl_4(H_2O)_2]$. The Re−O and Re−Cl distances are typical of values reported for similar complexes,[12] and the Re−Re−O angles [89.3(3)−90.3(3)°] are close to 90°. The corresponding angles involving the equatorial Cl^- ligands [103.6(1)−104.4(1)°] are much wider. This "bending back" of the chloride ligands away from the Re−Re bond and towards the axial sites leads to a marked non-linearity of the Re−Re−N (axial) units as evidenced by the Re4−Re3−N2 and Re3−Re4−N1 angles of 163.2(3) and 163.6(4)°, respectively.

Reaction of $[Rh_2(O_2CCH_3)_4]$ with **1** also produced crystals of a zig-zag polymeric chain compound with alternating triply bonded $Re_2^{III,III}$ and singly bonded $Rh_2^{II,II}$ units (Figure 4, c). A diagram of the unit $[\{cis\text{-}Re_2Cl_2(dppm)_2(O_2CC_5H_4N\text{-}4)_2\}\{Rh_2(O_2CCH_3)_4\}]$ is shown in Figure 6. Selected bond lengths and angles are provided in Table 4. The metrical parameters involving the triply bonded dirhenium units are similar to those observed in analogous complexes. The two sets of Rh−Rh distances [2.417(6) and 2.392(5) Å] observed in the crystal structure are both typical of singly bonded Rh_2^{4+} units with axial nitrogen donor ligands.[11] The axial Rh−N distances are 2.27(4) and 2.22(2) Å. The Rh1−Rh1′−N1 and Rh2−Rh2′−N2 angles are much closer to linearity at 177.6(7) and 176.3(7)° in complex **6** while the corresponding angles in complex **5** are significantly smaller.

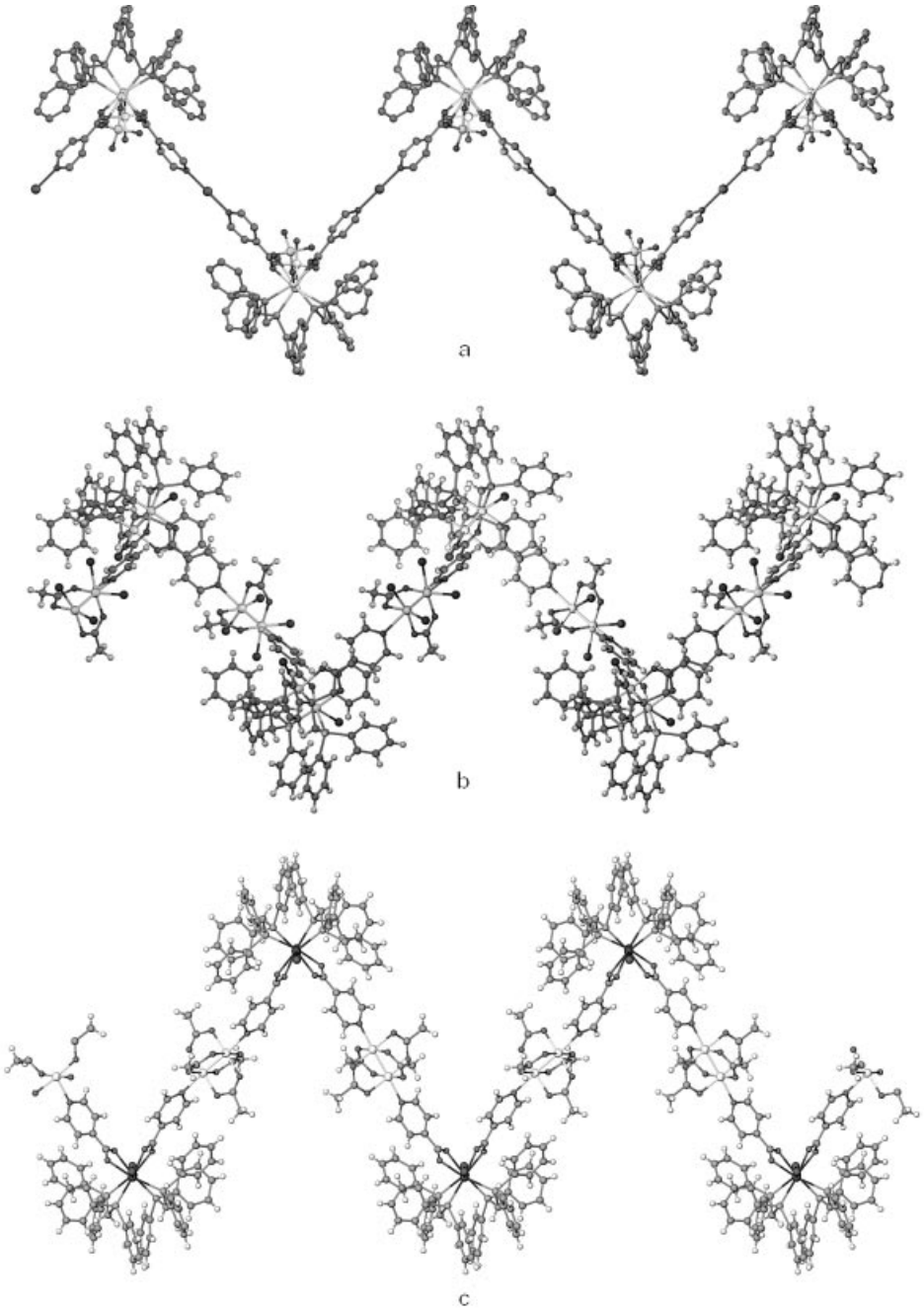

Figure 4. Graphical representation of the zig-zag patterns of the polymeric structures of complexes **4** (a), **5** (b), and **6** (c)

The crystal packing of compounds **2**−**6** share a common interesting feature, namely the phenyl groups of the dppm ligands from the neighboring molecules are engaged in close phenyl−phenyl contacts.[13] A representative example of the packing of Re_2/Zn squares in complex **3** is shown in Figure 7. Such arrangements create a cavity in the crystal lattice in which several solvent molecules are trapped during crystallization.

As documented here, self-assembly the reactions of **1** with *cis* and *trans* disposed linkers can yield discrete cyclic structures or polymers. The rationale for the formation of low-nuclearity species is based solely on the entropy factor. There is also a slight favorable enthalpic contribution for the stabilization of the cyclic structures versus the open-frame oligomers, as the former involves more metal−ligand interactions. Finally, the formation of the heterometallic squares **2** and **3** as the major products, rather than smaller or larger sized rings, is presumably a consequence of the ring-strain of the metallacyclophane. Having stated these points, why do the reactions of $Ag(O_3SCF_3)$, *cis*-$[Re_2Cl_4(O_2CCH_3)_2(H_2O)_2]$, and $[Rh_2(O_2CCH_3)_4]$ react with **1** to yield polymers instead of squares of larger dimensions? A common explanation is the role of concentration in the self-assembly reactions. Dilute solutions typically lead to cyclic

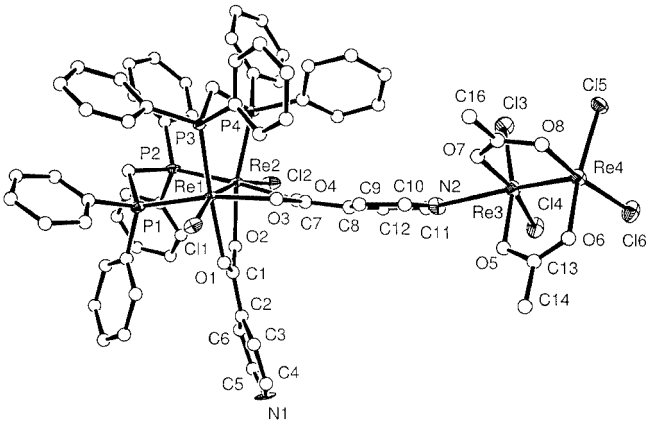

Figure 5. ORTEP representation of the repetitive neutral fragment [{*cis*-$Re_2Cl_2(dppm)_2(O_2CC_5H_4N\text{-}4)_2$}{*cis*-$Re_2Cl_4(O_2CCH_3)_2$}] in **5**·3($C_3H_6O$)·2($CH_2Cl_2$) with important atoms labeled. Thermal ellipsoids are at the 40% level except for the carbon and oxygen atoms which are represented as circles of arbitrary radius. Hydrogen atoms have been omitted for clarity

Table 3. Selected bond lengths [Å] and angles [deg] for **5**

Bond lengths			
Re1−Re2	2.3143(9)	Re2−P2	2.371(4)
Re4−Re3	2.2440(10)	Re2−P4	2.397(4)
Re3−N2	2.439(14)	Re2−Cl2	2.538(4)
Re4−N1	2.434(13)	Re3−O7	2.016(12)
Re1−O3	2.150(10)	Re3−O5	2.033(11)
Re1−O1	2.155(9)	Re3−Cl4	2.292(4)
Re1−P3	2.377(4)	Re3−Cl3	2.297(4)
Re1−P1	2.410(4)	Re4−O6	2.045(10)
Re1−Cl1	2.530(4)	Re4−O8	2.068(11)
Re2−O4	2.122(9)	Re4−Cl6	2.288(5)
Re2−O2	2.130(10)	Re4−Cl5	2.323(4)
Bond angles			
O3−Re1−O1	80.8(4)	Re4−Re3−Cl3	104.36(12)
O3−Re1−Re2	88.0(3)	Cl6−Re4−Cl5	93.42(17)
O3−Re1−Cl1	83.4(3)	O6−Re4−N1	78.0(5)
O1−Re1−Cl1	81.7(3)	O8−Re4−N1	78.6(5)
Re2−Re1−Cl1	167.90(10)	Cl6−Re4−N1	87.0(4)
O4−Re2−O2	79.8(4)	Cl5−Re4−N1	87.8(3)
O4−Re2−Cl2	83.4(3)	O7−Re3−O5	89.1(5)
O2−Re2−Cl2	80.8(3)	O7−Re3−Re4	89.3(3)
Re1−Re2−Cl2	167.01(10)	O5−Re3−Re4	89.9(3)
O6−Re4−O8	87.1(5)	O7−Re3−Cl4	166.7(3)
O6−Re4−Re3	89.6(3)	O5−Re3−Cl4	88.3(4)
O8−Re4−Re3	90.3(3)	O7−Re3−Cl3	86.8(4)
O6−Re4−Cl6	90.0(3)	O8−Re4−Cl5	86.0(3)
Cl4−Re3−Cl3	92.44(17)	O7−Re3−N2	78.7(5)
Re3−Re4−Cl6	103.81(12)	O5−Re3−N2	78.4(5)
Re3−Re4−Cl5	103.64(11)	Re3−Re4−N1	163.6(4)
Re4−Re3−Cl4	103.73(12)	Re4−Re3−N2	163.2(3)

products whereas concentrated solutions produce polymers. However, we found no evidence of lower nuclearity products, regardless of the concentrations of the precursors. Polymer formation may occur because squares of larger dimensions would require many solvent molecules to crystallize in the void space. Close-packed polymers also contain solvent molecules, but the packing of larger squares is expected to be much less efficient.

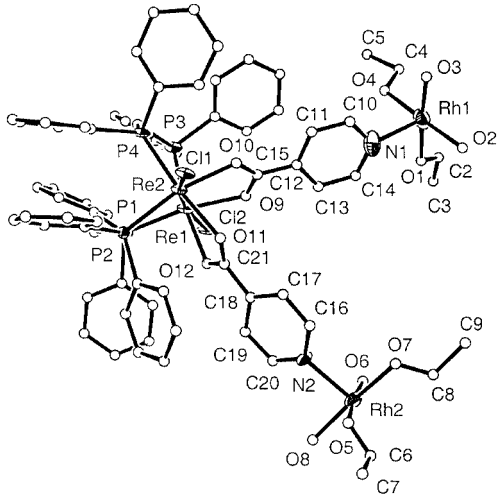

Figure 6. ORTEP representation of the repetitive neutral fragment [{*cis*-$Re_2Cl_2(dppm)_2(O_2CC_5H_4N\text{-}4)_2$}{$Rh_2(O_2CCH_3)_4$}] in **6**·1.5($C_3H_6O$)·2($CH_2Cl_2$)·$H_2O$ with important atoms labeled. Thermal ellipsoids are at the 40% level except for the carbon and oxygen atoms which are represented as circles of arbitrary radius. Hydrogen atoms have been omitted for clarity

Table 4. Selected bond lengths [Å] and angles [deg] for **6**

Bond lengths			
Re1−Re2	2.3425(15)	Re2−P2	2.438(6)
Rh1−Rh1	2.417(6)	Rh1−O2	2.02(3)
Rh2−Rh2	2.392(5)	Rh1−O4	2.02(3)
Re1−P1	2.408(7)	Rh1−O1	2.09(3)
Re1−P3	2.434(7)	Rh1−O3	2.10(3)
Re1−O12	2.165(18)	Rh1−N1	2.27(4)
Re1−O9	2.193(15)	Rh2−N2	2.22(2)
Re1−Cl2	2.529(6)	Rh2−O5	2.02(4)
Cl1−Re2	2.551(6)	Rh2−O7	2.04(3)
Re2−O10	2.179(17)	Rh2−O8	2.08(2)
Re2−O11	2.211(17)	Rh2−O6	2.09(3)
Re2−P4	2.407(7)		
Bond angles			
O12−Re1−O9	79.6(7)	P1−Re1−P3	95.7(2)
O12−Re1−Re2	88.2(5)	Re2−Re1−Cl2	166.81(19)
O9−Re1−Re2	86.1(4)	O2−Rh1−O1	88.0(12)
O12−Re1−P1	93.3(5)	O4−Rh1−O1	90.3(12)
O9−Re1−P1	169.6(5)	O2−Rh1−O3	87.7(16)
Re2−Re1−P1	101.48(15)	O4−Rh1−O3	93.9(17)
O12−Re1−P3	169.8(5)	N1−Rh1−Rh1	176.3(7)
O9−Re1−P3	90.8(5)	N2−Rh2−Rh2	177.6(7)

Concluding Remarks

The results of this study demonstrate the feasibility of preparing both discrete cyclic products and open-chain polymers based on the self-assembly of triply-bonded dirhenium units with various inorganic precursors. Dirhodium

Figure 7. Packing diagram of the Re_2/Zn molecular squares in the crystal structure of complex **3**

complexes with isonicotinate ligands as well as 4-cyanobenzoate groups have been prepared recently and it appears that this will be a generally useful method for preparing mixed-metal clusters.[14] The title compound **1** provides access to different types of heterometallic structures, and its reactions illustrate the usefulness of such molecules for incorporating electron-rich metal−metal bonded complexes into cyclic and acyclic architectures that contain a second type of metal site.[15]

Experimental Section

Solvents were dried by conventional methods, distilled from over nitrogen and deoxygenated prior to use. The starting materials *cis*-$[Re_2Cl_2(dppm)_2(O_2CC_5H_4N\text{-}4)_2]$,[7] *cis*-$[Re_2Cl_4(O_2CCH_3)_2(H_2O)_2]$,[16] $[Rh_2(O_2CCH_3)_4]$[17] were synthesized by literature methods. Silver triflate and zinc chloride were purchased from Aldrich and used without further purification. Infrared spectra were recorded in the range 400−4000 cm^{-1} using a Nicolet 470 FT-IR spectrometer as Nujol mull samples suspended between KBr plates. Elemental microanalyses were performed by Dr. H. D. Lee of the Purdue University Microanalytical Laboratory.

Synthesis of [{*cis*-$Re_2(O_3SCF_3)_2(dppm)_2(O_2CC_5H_4N\text{-}4)_2$}{Pt(dbbpy)}]$_2(O_3SCF_3)_4$ (2): A mixture of *cis*-$[Re_2Cl_2(dppm)_2(O_2CC_5H_4N\text{-}4)_2]$ (0.095 g, 0.07 mmol) and 0.052 g (0.07 mmol) of $[Pt(dbbpy)(O_3SCF_3)_2]$ was stirred in CH_2Cl_2 for 8−10 h. The resultant red solution was then concentrated and treated with diethyl ether to yield a solid that was collected by filtration, washed with fresh diethyl ether (3 × 5 mL) and dried in vacuo. Single crystals were grown by slow diffusion of Et_2O into a solution of **2** in CH_2Cl_2. Yield: 34 mg (42%). ^1H NMR (δ in $CDCl_3$): 5.05 and 6.50 (m, 4 H, -CH_2- of dppm); 6.8−7.2, 7.42, 7.60 (m, 40 H, Ph of dppm); 8.01 and 8.80 (m, 8 H, isonicotinate), 8.19, 8.28, 9.42 (m, 6 H, aromatic, dbbpy), 1.45 (m, 18 H, CH_3 of dbbpy) ppm. $^{31}P\{^1H\}$ NMR (δ in $CDCl_3$): −9.88 ppm.

Synthesis of [{*cis*-$Re_2Cl_2(dppm)_2(O_2CC_5H_4N\text{-}4)_2$}{$ZnCl_2$}]$_2$ (3): A CH_3OH solution (10 mL) of $ZnCl_2$ (5 mg, 0.04 mmol) was carefully layered over a solution of 1,2-dichloroethane (10 mL) that contained *cis*-$Re_2Cl_2(dppm)_2(O_2CC_5H_4N\text{-}4)_2$ (50 mg, 0.03 mmol). After 7 days, a crop of bright-red crystals was collected by filtration, washed with methanol (3 × 5 mL) followed by dichloromethane (3 × 5 mL) and dried in vacuo. Yield: 48 mg (87%). $C_{67}H_{64}Cl_8N_2O_5P_4Re_2Zn$ (i.e. **2**·$2C_2H_4Cl_2$·CH_3OH): calcd. (%) C 44.15, N 1.54, H 3.54, Cl 15.56; found C 44.01; N 1.52, H 3.51, 15.07.

Synthesis of [{*cis*-$Re_2(OReO_3)_2(dppm)_2(O_2CC_5H_4N\text{-}4)_2$}{Ag·$ReO_4$}] (4): A CH_3OH solution of AgO_3SCF_3 (10 mg, 0.04 mmol) was layered over a solution of *cis*-$[Re_2Cl_2(dppm)_2(O_2CC_5H_4N\text{-}4)_2]$ (50 mg, 0.03 mmol) in 1,2-dichloroethane (10 mL). The Schlenk-tube was then wrapped with foil to avoid light and stored in a refrigerator. After 7 days, a small quantity of block-shaped crystals of **2** had formed along with a gray precipitate. The crystals were separated from the solid, washed with methanol (3 × 5 mL) followed by dichloromethane (3 × 5 mL) and dried in vacuo. Yield: 16 mg (21%). $C_{62}H_{52}AgN_2O_{16}P_4Re_5$: calcd. C 33.19, N 1.25, H 2.34; found C 32.92; N 1.28, H 2.32.

Synthesis of [{*cis*-$Re_2Cl_2(dppm)_2(O_2CC_5H_4N\text{-}4)_2$}{*cis*-$Re_2Cl_4(O_2CCH_3)_2$}] (5): An acetone solution (10 mL) of *cis*-$[Re_2Cl_4(O_2CCH_3)_2(H_2O)_2]$ (25 mg, 0.04 mmol) was carefully layered over a dichloromethane solution of *cis*-$[Re_2Cl_2(dppm)_2(O_2CC_5H_4N\text{-}4)_2]$ (50 mg, 0.03 mmol). After 2 days, the dark blue crystals that had formed were collected by filtration, washed with acetone (3 × 5 mL) followed by dichloromethane (3 × 5 mL) and dried in vacuo. Yield: 66 mg (92%). $C_{66}H_{58}Cl_6N_2O_8P_4Re_4$: calcd. (%) C 37.95, N 1.34, H 2.80; Cl 10.18; found C 37.65; N 1.31, H 2.73, Cl 10.03.

Synthesis of [{*cis*-$Re_2Cl_2(dppm)_2(O_2CC_5H_4N\text{-}4)_2$}{$Rh_2(O_2CCH_3)_4$}] (6): An acetone solution (10 mL) of $[Rh_2(O_2CCH_3)_4]$ (17 mg, 0.04 mmol) was carefully layered over a dichloromethane solution of *cis*-$[Re_2Cl_2(dppm)_2(O_2CC_5H_4N\text{-}4)_2]$ (50 mg, 0.03 mmol). After 7 days, the resultant red crystals were collected by filtration, washed with acetone (3 × 5 mL) and dichloromethane (3 × 5 mL), and dried in vacuo. Yield: 56 mg (86%). $C_{70}H_{64}Cl_2N_2O_{12}P_4Re_2Rh_2$: calcd. (%) C 44.29, N 1.48, H 3.40; found C 44.11; N 1.56, H 3.27.

X-ray Crystallography: Crystals of **3**−**6** were harvested directly from the slow diffusion reactions as described in the synthesis section. Single-crystal X-ray intensities were collected at 110(2) K on a Bruker SMART CCD based X-ray diffractometer with 1.5 kW graphite monochromated Mo-K_α radiation (λ = 0.71073 Å). Data reduction, cell-refinement, and corrections for Lorentz and polarization effects were carried out with the program SAINT.[18] Semi-empirical absorption corrections were carried out with the program SADABS.[19] The structures were solved and refined using X-SEED,[20] a graphical interface to SHELX.[21] Additional crystallographic calculations were performed by the programs PLATON[22] and PARST.[23] The hydrogen atoms were refined in a riding mode with values of U_{eq} that were 1.2 times the U_{eq} for the heavy atoms to which they are bonded. Experimental details and pertinent crystallographic data for complexes **3**−**6** are summarized in Table 5.

[{*cis*-$Re_2Cl_2(dppm)_2(O_2CC_5H_4N\text{-}4)_2$}{$ZnCl_2$}]$_2$·10($C_2H_4Cl_2$)·11($CH_3OH$)·($H_2O$) [3·10($C_2H_4Cl_2$)·11($CH_3OH$)·($H_2O$)]: The data were collected using ω-scans in the range $1.67 < \theta < 27.82°$. The detector to crystal distance was set at 60 mm. Exposure times of 20 s per frame and scan widths of 0.3° were used throughout the data collection. The fact that the beta angle is close to 90° combined with the large R-merge value indicated possible pseudo-

Table 5. Crystallographic data for complexes **3**−**6**

	3·10$C_2H_4Cl_2$·11CH_3OH·H_2O	**4**·1.5($C_2H_4Cl_2$)·2(CH_3OH)	**5**·3(C_3H_6O) ·2(CH_2Cl_2)	**6**·1.5(C_3H_6O)·2(CH_2Cl_2)·H_2O
Formula	$C_{155}H_{190}Cl_{28}N_4O_{20}P_8Re_4Zn_2$	$C_{67}H_{66}AgCl_3N_2O_{18}P_4Re_5$	$C_{77}H_{80}Cl_{10}N_2O_{11}P_4Re_4$	$C_{76.50}H_{79}Cl_6N_2O_{14.5}P_4Re_2Rh_2$
Molecular mass	4545.01	2456.32	2432.61	2173.22
Crystal system	monoclinic	monoclinic	orthorhombic	monoclinic
Space group	$P2_1/n$ (No. 14)	$P2_1/c$ (No. 14)	*Pbcn* (No. 60)	$P2_1/n$ (No. 14)
a [Å]	16.289(3)	19.504(4)	23.150(5)	16.209(3)
b [Å]	35.117(7)	16.407(3)	24.220(5)	38.889(8)
c [Å]	17.001(3)	24.360(5)	33.300(7)	17.363(4)
β [deg]	90.08(3)	92.68(3)		90.42(3)
V [Å^3]	9725(3)	7787(3)	18671(6)	10945(4)
Z	2	4	8	4
$\rho_{calcd.}$ [g/cm^3]	1.552	2.095	1.731	1.319
μ (Mo-K_α) [mm^{-1}]	3.229	8.238	5.577	2.753
F(000)	4528	4636	9392	4280
Reflections collected	56099	51822	81011	74227
Independent	21289	14162	13495	13984
Observed [$I > 2\sigma(I)$]	12028	7692	8618	6996
No. of variables	952	508	868	585
R_1[a]	0.092	0.093	0.092	0.127
wR_2[b]	0.211	0.247	0.189	0.331
Goodness-of-fit	1.017	1.025	1.144	1.020

[a] $R1 = \Sigma||F_o| - |F_c||/\Sigma F_o$ with $F_o^2 > 2\sigma(F_o^2)$. [b] $wR_2 = [\Sigma w(|F_o^2| - |F_c^2|)^2/\Sigma|F_o^2|^2]^{1/2}$.

merohedral twinning of the crystal. A search for possible twin laws was carried out, but none of them reduced the *R*-factor appreciably. As the final discrepancy indices of both R_1 and R_{int} were small for a potentially twinned data set, we surmised that the major contribution to the integrated data was from one component of the twin and therefore a twin correction would not improve the model significantly. Disordered solvent molecules with fractional site occupancies were modeled with restraints. All non-hydrogen atoms except the carbon and oxygen atoms of the methanol and water molecules were refined anisotropically.

[{*cis*-$Re_2(OReO_3)_2(dppm)_2(O_2CC_5H_4N$-4)$_2$}{Ag·$ReO_4$}]·1.5($C_2H_4Cl_2$)·2-($CH_3OH$) [4·1.5($C_2H_4Cl_2$)·2($CH_3OH$)]: Exposure times of 25 s per frame and scan widths of 0.3° were used throughout the data collection. The data were collected using ω-scans in the θ range 1.53 to 25.35°. The numerous heavy metal atoms resulted in the crystal exhibiting a large absorption coefficient. Unfortunately, the weak nature of the diffraction prevented the use of very small crystal that would minimize the effects of absorption. The isolated $[ReO_4]^-$ ions are disordered over two positions and were modeled using two components with restraints on the Re−O and O···O distances and site occupancies. All the non-hydrogen atoms except the carbon and oxygen atoms were refined anisotropically.

[{*cis*-$Re_2Cl_2(dppm)_2(O_2CC_5H_4N$-4)$_2$}{*cis*-$Re_2Cl_4(O_2CCH_3)_2$}]·3-($C_3H_6O$)·2($CH_2Cl_2$) [5·3($C_3H_6O$)·2($CH_2Cl_2$)]: The data were collected using ω-scans in the range $1.22 < \theta < 23.34°$. The diffraction patterns were indexed using a primitive orthorhombic cell, and the structure was solved and refined in the space group *Pbcn*. A disordered dichloromethane solvent molecule was modeled using two components with restraints on the C−Cl and Cl···Cl distances and site occupancies for the two fragments set to 0.5 each. In the final cycles of refinement, all non-hydrogen atoms, except those belonging to solvent molecules, were refined anisotropically.

[{*cis*-$Re_2Cl_2(dppm)_2(O_2CC_5H_4N$-4)$_2$}{$Rh_2(O_2CCH_3)_4$}]·1.5-($C_3H_6O$)·2($CH_2Cl_2$)·$H_2O$ [6·1.5(C_3H_6O)·2(CH_2Cl_2)·H_2O]: The crystal selected for data collection was removed from the solvent and quickly placed in a cold-stream to prevent decay. The detector-to-crystal distance was set at 60 mm. Exposure times of 40 s per frame and scan widths of 0.3° were used throughout the data collection. The data were collected using ω-scans in the θ range 1.57 to 23.14°. The diffraction patterns were indexed using a primitive monoclinic cell. The space group $P2_1/n$ was chosen on the basis of the systematic absences in the diffraction pattern. In the final cycles of refinement the Re, Cl, P, and O atoms belonging to the coordination polymer were refined anisotropically. Anisotropic refinement of carbon atoms and the atoms belonging to guest molecules resulted in these atoms having non-positive definite displacement parameters.

Acknowledgments

K. R. D. gratefully acknowledges the Welch Foundation and the National Science Foundation for a PI Grant (CHE-9906583) and for equipment grants to purchase the CCD X-ray equipment (CHE-9807975). K. R. D. also thanks Johnson-Matthey for a generous loan of rhodium trichloride.

[1] [1a] O. Ermer, *Adv. Mater.* **1991**, *3*, 608, and references therein. [1b] A. Aumuller, P. Erk, G. Klebe, S. Hünig, J. U. von Schütz, H. P. Werner, *Angew. Chem. Int. Ed. Engl.* **1986**, *25*, 740.

[2] C. S. Campos-Fernández, J. R. Galán-Mascarós, B. W. Smucker, K. R. Dunbar, *Eur. J. Inorg. Chem.* **2003**, 988, and references cited therein.

[3] [3a] U. Hahn, M. Gorka, F. Vogtle, V. Vicinelli, P. Ceroni, M. Maestri, V. Balzani, *Angew. Chem. Int. Ed.* **2002**, *41*, 3595. [3b] V. Balzani, P. Ceroni, A. Juris, M. Venturi, S. Campagna, F. Puntoriero, S. Serroni, *Coord. Chem. Rev.* **2001**, *219*, 545, and references cited therein.

[4] [4a] M. Abrantes, A. Valente, M. Pillinger, I. S. Goncalves, J. Rocha, C. C. Romao, *J. Catal.* **2002**, *209*, 237. [4b] R. Tannenbaum, *J. Mol. Catal. A: Chem.* **1996**, *107*, 207. [4c] M. Fujita, Y. J. Kwon, S. Washizu, K. Ogura, *J. Am. Chem. Soc.* **1994**, *116*, 1151.

[5] [5a] F. A. Cotton, C. Lin, C. A. Murillo, *Acc. Chem. Res.* **2001**, *34*, 759 and references cited therein. [5b] J. K. Bera, R. Clérac, P. E. Fanwick, R. A. Walton, *J. Chem. Soc., Dalton Trans.* **2002**, 2168. [5c] J. K. Bera, P. Angaridis, F. A. Cotton, M. A.

Petrukhina, P. E. Fanwick, R. A. Walton, *J. Am. Chem. Soc.* **2001**, *123*, 1515. [5d] R. H. Cayton, M. H. Chisholm, J. C. Huffman, E. B. Lobkovsky, *J. Am. Chem. Soc.* **1991**, *113*, 8709.
[6] [6a] S.-M. Kuang, P. E. Fanwick, R. A. Walton, *Inorg. Chem.* **2002**, *41*, 1036; *Inorg. Chem.* **2002**, *41*, 147; *Inorg. Chem.* **2001**, *40*, 5682; *Inorg. Chem.* **2000**, *39*, 2968.
[7] J. K. Bera, B. W. Smucker, R. A. Walton, K. R. Dunbar, *Chem. Commun.* **2001**, 2562.
[8] For other references to the use of Ag^{I} as a linking cation see: [8a] D. Braga, M. Polito, M. Bracaccini, D. D'Addario, E. Tagliavini, D. M. Proserpio, F. Grepioni, *Chem. Commun.* **2002**, 1080. [8b] R. Schneider, M. W. Hosseini, J.-M. Plainex, A. De Cian, J. Fisher, *Chem. Commun.* **1998**, 1625.
[9] A. R. Cutler, D. R. Derringer, P. E. Fanwick, R. A. Walton, *J. Am. Chem. Soc.* **1988**, *110*, 5024.
[10] [10a] J. K. Bera, T.-T. Vo, R. A. Walton, K. R. Dunbar, *Polyhedron*, in press. [10b] Y. Ding, S. S. Lau, P. E. Fanwick, R. A. Walton, *Inorg. Chim. Acta* **2000**, *300–302*, 505.
[11] F. A. Cotton, E. V. Dikarev, M. A. Petrukhina, M. Schmitz, P. J. Stang, *Inorg. Chem.* **2002**, *41*, 2903, and references cited therein.
[12] F. A. Cotton, R. A. Walton, *Multiple Bonds Between Metal Atoms*, 2nd ed., Clarendon Press, Oxford, **1993**.
[13] I. Dance, M. Scudder, *Chem. Eur. J.* **1996**, *2*, 481.
[14] S. L. Schiavo, F. Nicolò, G. Tresoldi, P. Piraino, *Inorg. Chim. Acta* **2003**, *343*, 351.
[15] J. K. Bera, J. Bacsa, K. R. Dunbar, unpublished work.
[16] A. R. Chakravarty, F. A. Cotton, A. R. Cutler, R. A. Walton, *Inorg. Chem.* **1986**, *25*, 3619.
[17] G. A. Rempel, P. Legzdins, H. Smith, G. Wilkinson, *Inorg. Synth.* **1972**, *13*, 87.
[18] *SAINT*, Program for area detector absorption correction, Siemens Analytical X-ray Instruments Inc., Madison, WI 53719, USA, **1994–1996**.
[19] G. M. Sheldrick, *SADABS*, Program for Siemens area detector absorption correction, Univ. of Göttingen, Germany, **1996**.
[20] L. J. Barbour, *X-Seed*, Graphical interface to SHELX-97 and POV-Ray, **1999** (http://www.x-seed.net).
[21] G. M. Sheldrick, *SHELXS-97, A Program for Crystal Structure Solution,* Univ. of Göttingen, Germany, **1997**. G. M. Sheldrick, *SHELXL-97, A Program for Crystal Structure Refinement,* Univ. of Göttingen, Germany, **1997**.
[22] A. L. Spek, *PLATON*, University of Utrecht, The Netherlands, **2001**.
[23] *PARST:* M. Nardelli, *J. Appl. Crystallogr.* **1995**, *28*, 659.

Received May 6, 2003
Early View Article
Published Online November 6, 2003

